Available online at BCREC Website: http://bcrec.undip.ac.id

Bulletin of Chemical Reaction Engineering & Catalysis, 10 (2), 2015, 175-184

Research Article

Thermal Behavior and Hydrogen Production of Methanol Autothermal Reforming Performed Using Oxygen Enrichment and $Cu/ZnO/Al_2O_3/Cr_2O_3/CeO_2$ Catalyst

Donny Lesmana[1,2], **Ho-Shing Wu**[1,*]

[1] *Department of Chemical Engineering and Materials Science, Yuan Ze University, 135 Yuan Tung Road, Chung Li, Taoyuan, 32003, Taiwan*
[2] *Department of Chemical Engineering, Faculty of Engineering, Universitas Lampung, 1 Soemantri Brojonegoro, Rajabasa, Bandar Lampung, 35145, Indonesia*

Received: 29th August 2014; Revised: 19th March 2015; Accepted: 19th March 2015

Abstract

A fixed-bed reactor designed for the autothermal reforming (ATR) of methanol under adiabatic conditions was constructed to experimentally determine the profile of temperature and catalyst activity generated using the $Cu/ZnO/Al_2O_3/Cr_2O_3/CeO_2$ catalyst. The effect of oxygen enrichment in this experiment was investigated, and the experimental results showed that an increase in oxygen concentration correlated with an increase in the temperature of the catalytic bed; by contrast, this increase in oxygen concentration resulted in a reduction of the startup time of the catalyst. Moreover, the reaction temperature was determined to vary with the position within the catalytic fixed bed. © 2015 BCREC UNDIP. All rights reserved

Keywords: Autothermal Reforming; Methanol; Fixed Bed; Oxygen Enrichment; Hydrogen

How to Cite: Lesmana, D., Wu, H.S. (2015). Thermal Behavior and Hydrogen Production of Methanol Autothermal Reforming Performed Using Oxygen Enrichment and $Cu/ZnO/Al_2O_3/Cr_2O_3/CeO_2$ Catalyst. *Bulletin of Chemical Reaction Engineering & Catalysis*, 10 (2), 175-184. (doi:10.9767/bcrec.10.2.7228.175-184)

Permalink/DOI: http://dx.doi.org/10.9767/bcrec.10.2.7228.175-184

1. Introduction

Hydrogen can be produced from methanol, natural gas, and ethanol. Methanol is simply the easiest to convert H_2 because its boiling point is low and it is safe to handle and store [1, 2], and also because methanol is sulfur-free, and it can be activated at low temperatures (<300 °C) [3]. Methanol features a high hydrogen-carbon ratio and no C–C bonds, which minimizes the risk for coke formation. Moreover, methanol can be obtained from biomass [4, 5]. Hydrogen can be produced from methanol by using various catalytic processes: steam reforming (SRM), partial oxidation (POM), and oxidative steam reforming (OSRM, Equation (1)); OSRM, which is also called autothermal reforming (ATR), is a combination of SRM and POM [6, 7].

$$CH_3OH + (1\text{-}\alpha)\ H_2O + 0.5\alpha\ O_2 \longrightarrow CO_2 + (3\text{-}\alpha)\ H_2$$
$$(\Delta H = 49.5\text{-}241.8\alpha \text{ kJ/mol},\ 0 \leq \alpha \leq 1) \qquad (1)$$

---

* Corresponding Author.
E-mail: cehswu@saturn.yzu.edu.tw (H.S. Wu);
lesmanadonny38@yahoo.co.id (D. Lesmana)
Tel: +886-3-4638800#2564, Fax : +886-3-4631181

The overall heat of the reaction depends on the value of a, the molar ratio of oxygen to methanol, which directly influences the thermal properties of the ATR system and also the hydrogen concentration [8, 9].

The ATR process, which requires no external heat generation [6, 10] and can run adiabatically, has not been studied extensively [11]. The ATR process can reach operating temperatures quickly; however, to enable a cold catalytic reactor to reach operating temperatures >250 °C within a few seconds, the rest of the plant must be synchronized and the reaction parameters must be carefully controlled [12]. Simulations have been used to investigate several strategies developed for cold-start ATR reactions [13]. However, the temperature profile of the initial reaction phase of the ATR reaction must be characterized because these data are required for further developing and explaining the heat transfer that occurs in a fixed-bed reactor.

Air separation refers to the ability to control the ratio of oxygen to nitrogen. The use of membranes allows nitrogen to be partially removed from air and thus obtain oxygen-enriched air [14, 15] in which oxygen can reach a concentration of >21 vol.%. The enriched oxygen could influence the temperature characteristics and the catalytic activity in the ATR. Moreover, the presence of nitrogen in the air can inhibit the reaction or lead to the reaction not being completed. Nitrogen lowers the reaction temperature and increases energy losses. This study demonstrates this effect by conducting experiments under conditions in which the oxygen concentration was higher than the typical concentration of oxygen in the air. By extending and contracting the combustion zone by means of oxygen enrichment and depletion, the products of the partial-oxidation combustion regime can be modified to exhibit favorable characteristics; specifically, the water–gas shift reaction used for reducing the amount of water in the product not only increases the hydrogen (H_2) yield, but also reduces carbon monoxide (CO) concentrations [16]. If oxygen-enriched air is used in the partial-oxidation combustion, the diluting effect of nitrogen can be diminished [17]. Even this, the air is always used in the autothermal reforming reaction because its price is cheaper than pure oxygen.

This study was aimed to understand how oxygen enrichment affects the temperature characteristics and catalyst activity in the ATR reaction. Elucidating the ATR temperature characteristics can help with investigations into the ability of the ATR catalyst to enable rapid startup, which should facilitate further studies on fuel cells (FC).

2. Materials and Methods

2.1. Materials

Methanol (99%) was purchased from Echo Chemical (Miaoli, Taiwan), aluminum nitrate-9-hydrate (99%) from J.T. Baker (Mexico, USA), and copper nitrate-2.5-hydrate, zinc nitrate-6-hydrate, chromium nitrate-6-hydrate, cerium nitrate-6-hydrate, and oxalic acid (all 99%) from R.D.H (Seelze, Germany), and oxygen (99.99%) from Ming Yang Gas (Taoyaun, Taiwan). The reagents were used as supplied.

2.2. Preparation of Catalyst

The preparation of catalysts was reported in our previous study [7, 18, 19]. Catalyst-precursor solutions were prepared by adding $Cu(NO_3)_2.2.5H_2O_{(s)}$ (11.7 g), $Zn(NO_3)_2.6H_2O_{(s)}$ (11.7 g), $Al(NO_3)_3.9H_2O_{(s)}$ (2.56 g), $Cr(NO_3)_2.6H_2O_{(s)}$ (0.43 g), and $Ce(NO_3)_3.6H_2O_{(s)}$ (0.90 g) into flasks containing ethanol (100 ml, -5 °C), and the solutions were stirred until the compounds dissolved. Each precursor solution was reacted with 20%-excess oxalic acid. The initial pH of the precursor solution was measured to be 0.4 by using a pH meter (SP-701, Suntex, Taiwan). The precipitate ($Cu/ZnO/Al_2O_3/Cr_2O_3/CeO_2$ (42.9:42.9:7.14: 3.57:3.57 wt.%)) was subsequently filtered and washed with deionized water and then dried at 100 °C for 24 h. All precursors were then calcined under O_2 at a flow rate of 100 ml/min, by applying a programmed temperature regime [18] as depicted in Scheme 1, in which the time marked with " * " is holding time, and the others are heating time.

After the calcination reactions, the catalyst was ground into granules and 60-80-mesh cata-

$$\text{RT} \xrightarrow{30\ \text{min}} 150\,^{\circ}\text{C} \xrightarrow{25\ \text{min*}} 150\,^{\circ}\text{C} \xrightarrow{20\ \text{min}} 200\,^{\circ}\text{C} \xrightarrow{25\ \text{min*}} 200\,^{\circ}\text{C}$$

$$\xrightarrow{20\ \text{min}} 250\,^{\circ}\text{C} \xrightarrow{25\ \text{min*}} 250\,^{\circ}\text{C} \xrightarrow{20\ \text{min}} 300\,^{\circ}\text{C} \xrightarrow{3\ \text{h*}} 300\,^{\circ}\text{C}$$

Scheme 1. Programmed temperature regime for calcinations process lytic particles were sieved out. The catalyst was then reduced under a stream of 10% H_2/N_2 (100 cm^3/min), with the sample being heated from 25 to 300 °C at a rate of 5 °C /min, and then held at 300 °C for 3 h.

2.3. Measurement of Catalyst Activity

The experimental apparatus used was described in our previous work [19]. First, the $Cu/ZnO/Al_2O_3/Cr_2O_3/CeO_2$ catalysts were prepared as mentioned in Section 2.2. A mixture of methanol and deionized water (molar ratio of water/methanol (W/M) = 1.2, premixed) was introduced into an evaporator through a syringe pump (Cole Parmer, 79400 series, USA) at a rate of 2.4 cm^3/h. Air was injected into the evaporator at a flow rate of 15, 20 or 25 sccm (standard cubic centimeters per min) using a mass flow meter (5850 E series, Brooks, USA). The standard condition was 0 °C and 1 atm. Oxygen (99.99%) was introduced into the evaporator at a flow rate of 0, 1, or 2 sccm to obtain oxygen concentrations from 21% to 30% v/v (molar ratio of oxygen to methanol (O/C) = 0.27-0.46), and the weight hourly space velocity (WHSV) was operated at 6.22 h^{-1} (= $g_{feed}.h^{-1}$ g_{cat}^{-1}). This mixture (water, methanol, air, and oxygen) was then passed through an evaporator and heated to evaporate mixture to the gas phase. All experiments were conducted at a pressure of 1 atm and a temperature of 180-200 °C. The reactor outlet was heated using an electric heating tape to prevent condensation of the compounds in the gas.

Isopropanol (33 ml) was used to condense methanol and water in a condenser at -5 °C. After the reaction, the liquid was collected and the methanol content was determined by using a gas chromatograph (Shimadzu 14B, Japan) equipped with a flame ionization detector and the following chromatography parameters: a carrier gas was used in which nitrogen was the mobile phase (30 cm^3/min) and a mixture of hydrogen (0.9 kg/cm^2) and air (0.6 kg/cm^2) was the detector gas; a 7HK-G013-22 ZB-WAX column (length 30 m, I.D. 0.53 mm, film 1 μm) was used; and the oven temperature was held for 1 min at 45 °C and raised at a rate of 15 °C/min from 45 to 75 °C. The sample was withdrawn after 1 h.

The concentrations of H_2, CO, and CO_2 were measured using a gas chromatograph (Shimadzu 8A, Japan) equipped with a thermal-conductivity detector; in the carrier gas, helium was the mobile phase (30 cm^3/min), and a molecular sieve 13X column and a Chromosorb 120 column were used. The oven temperature was held at 100 °C for 3 min, increased from 100 to 160 °C (at a rate of 32 °C/min), and then held at 160 °C for 20 min. The sample was withdrawn after 1 h.

2.4. Measurement of Temperature Profiles

The catalyst was placed in a fixed-bed reactor (Figure 1) that was 1 cm in diameter and 15 cm long. The body of fixed-bed reactor was insulated using up to 1 kg of silicon-carbide cotton, covered with tape from the entrance of the reactive tube to the bottom of the catalytic bed, and then placed in an electrically heated furnace. The temperature was controlled using a microprocessor-based temperature controller equipped with a K-type thermocouple (Maxthermo, MC-2438, Taiwan).

Temperatures at T1, T2, T3, T4, and T5 were measured during the ATR reaction (Fig. 1). In the case of the thermocouple with 1 mm in diameter placed inside the catalytic bed (T3), the position of the thermocouple tip varied from x/L = 0.2-0.8; this represents the relative length of the catalytic bed, in which x denotes the distance between the upper limit of bed catalyst and the tip of the thermocouple to be immersed into the catalytic bed, and L is the height of catalytic bed. The catalytic bed contained approximately 0.2 g of 60-80-mesh catalyst particles, which equaled 20 mm of the height of catalytic bed.

First, the temperatures in the preheater (T1) and at the inlet point of the reactor (T2)

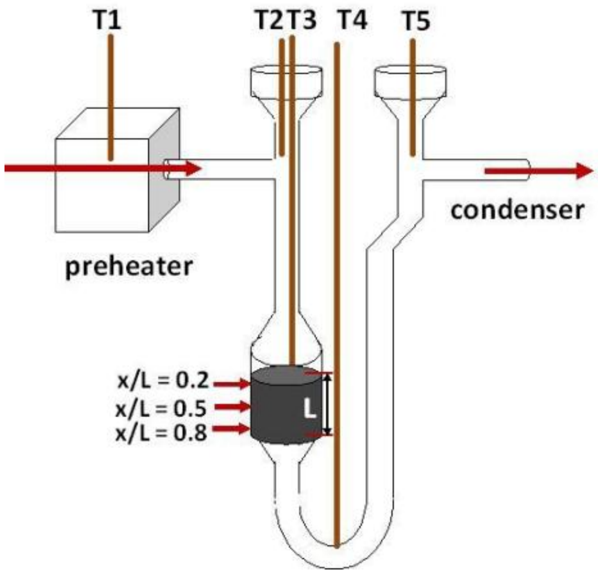

Figure 1. Schematic representation of the locations of the thermocouples in the fixed-bed reactor

were set to 180-200 °C, and then the catalytic bed (T3) was heated using a 1.2 kW heater until the bed reached the selected temperature of 180-200 °C, after which the temperatures on T3 and T4 were monitored for 120 min during the ATR reaction.

2.5. Mathematical Equation Used for Measuring Catalyst Activity

The compounds that were present after the oxidative-reforming reaction process was completed were methanol (M), water (W), hydrogen (H_2), carbon monoxide (CO), and carbon dioxide (CO_2). No other compounds were detected. The quantified contents can be expressed in Equations 2-4.

$$X_M(\%) = \frac{W_{M,0} - W_{M,unreacted}}{W_{M,0}} \text{ x } 100 \tag{2}$$

$$V_{H_2}(\%) = \frac{V_{H_2}}{V_{total}} \text{ x } 100 \tag{3}$$

$$V_{CO}(ppm) = \frac{V_{CO}}{V_{total}} \text{ x } 10^6 \tag{4}$$

where X_M denotes the methanol conversion, and V_{H2} and V_{CO} denote the volumetric concentrations of hydrogen and carbon monoxide, respectively. The term $W_{M,0}$ denotes the initial molar flow of methanol (mol/min), which was measured using gas chromatography. V_{total} denotes the total combined volumetric concentration of H_2, N_2, CO_2, and CO. The production rate per weight of the catalyst (mol/(min.g catalyst) is that the molar flow rate of hydrogen gas is divided by the weight of the catalyst.

3. Results and Discussion

In our previous study, Lesmana and Wu [18] reported that the catalytic performance of the ATR reaction conducted using a $Cu/ZnO/Al_2O_3/Cr_2O_3/CeO_2$ (42.9:42.9:7.14:3.57:3.57 wt.%) catalyst was high at a reaction temperature of 200 °C. After 50 h reaction time, the catalyst achieved a methanol conversion of 90% with the volume percentage of hydrogen gas, and the CO concentration as 48%, and 1000 ppm, respectively. The same catalyst composition was used in the studies described here.

3.1. Effect of Elevated Oxygen Concentrations on the Autothermal Reforming of Methanol

Polymeric membranes are widely used in commercial air separation [14], and oxygen can be readily enriched using polymeric membranes on board in the fuel processer. In this study, oxygen-enriched air was simulated by mixing air and pure oxygen. The effects of high oxygen concentrations at various starting temperatures was employed by using air at flow rates of 15 and 25 sccm and oxygen at flow rates of 0, 1 and 2 sccm as the feed in the ATR reaction (Figure 2). Hence, the oxygen concentration is different for each air flow (Figure 2). In case of 15 sccm, increasing the oxygen concentration enhanced the conversion of methanol because the reaction exothermal enthalpy calculated by Equation 1 is increased from -46.3 mol/mol to -107.2 kJ/mol so to increase the reaction temperature, but resulted in a decrement of the concentration of hydrogen because the coefficient (3-a) of producing hydrogen in Equation 1 is theoretically decreased. Moreover, the hydrogen reacted with the excess oxygen. Consequently, the amount of CO gas produced increased. Furthermore, the hydrogen-production rate was higher at 15 sccm than at 25 sccm, and high hydrogen-production rates were obtained at low oxygen concentrations (< 26%) and a high initial temperature (200 °C).

Figure 3 shows the effect of oxygen enrichment on the startup-time profile in the ATR process in relation to various airflow rates. The startup time was defined as the time required for T3 (x/L = 0.5) to reach the selected temperature of 200 °C. All the startup times were <20 s (Figure 4), and increasing the oxygen concentration (or the ratio of O/C in Figure 4) resulted in a reduction in startup time because of releasing more heat according to Eq. 1. This likely occurred because the release of the heat generated as a result of excess oxygen being present at a high airflow rate would lead to the burning of the catalyst under the initial conditions; the released heat would increase the temperature at the start oxidation, which would stimulate the catalyst and accelerate the reformation under initial conditions.

The results in Figure 5 show that the inlet temperature (T2) clearly increased during the startup of the ATR when the flow rate was 20 sccm. Increasing the inlet temperature of the reactant led to an increase in the reaction temperature and a decrease in the startup time (T3 = 200 ^{o}C) in the ATR reaction. The minimal startup time of 14 s was reached at a preheating temperature of approximately 200 °C, and the reaction was slow when the inlet temperature was the ambient temperature. Figure 5b presents the effects of oxygen concentrations in the air on the startup time in the ATR reaction; the minimal startup time was 12 s. This was likely because of additional heat being generated by the reaction of hydrogen with the oxygen, and the exothermal heat then accumulating on the catalyst surface and increasing the reactivity of the catalyst.

3.2. Effect of Temperature on the Heating up of the Catalyst under Initial Conditions

To determine the relationship between the position and the temperature in the catalytic bed, the effects of various temperatures on T1, T2, and T3 were tested. T3 and T4 were monitored and recorded in this ATR reaction. Figure 6 shows the temperature profile of T3 and T4 in the catalytic bed measured using distinct inlet temperatures with T1 = T2; T3 and T4 were measured over the length of the catalytic bed at x/L = 0.2, 0.5, and 0.8. T1 and T2 were controlled at selected temperatures between 180 and 200 °C, and the initial temperature at T3 was the same as the selected of temperature of T1 and T2. T3 and T4 were observed for 120 min on stream because the result for long time on stream (> 50 h) was reported in the previous work [18].

Figures 6a-6c show that a sharp peak corresponding to T3 appeared at <20 min when the temperature was increased and remained mostly stable after the reaction has proceeded for 40 min. The maximal temperature was around 350 °C, and the stable temperature was around 300 °C when x/L was <0.5. T4 exhibited the same trend, and the maximal temperature was approximately 240 °C. The temperature increased at the beginning of the ATR process because the partial oxidation (POX) mode is initiated by the contact with oxygen (air) between the fuel over the heated catalytic bed; moreover, because the exothermic reaction further heats the catalytic bed and the catalyst is still fresh, the activity of catalyst is extremely high, and this results in the temperature during the initial reaction being high [12, 13]. The variation of the temperature (T3 at x/L = 0.8) strongly depended on the initial T3.

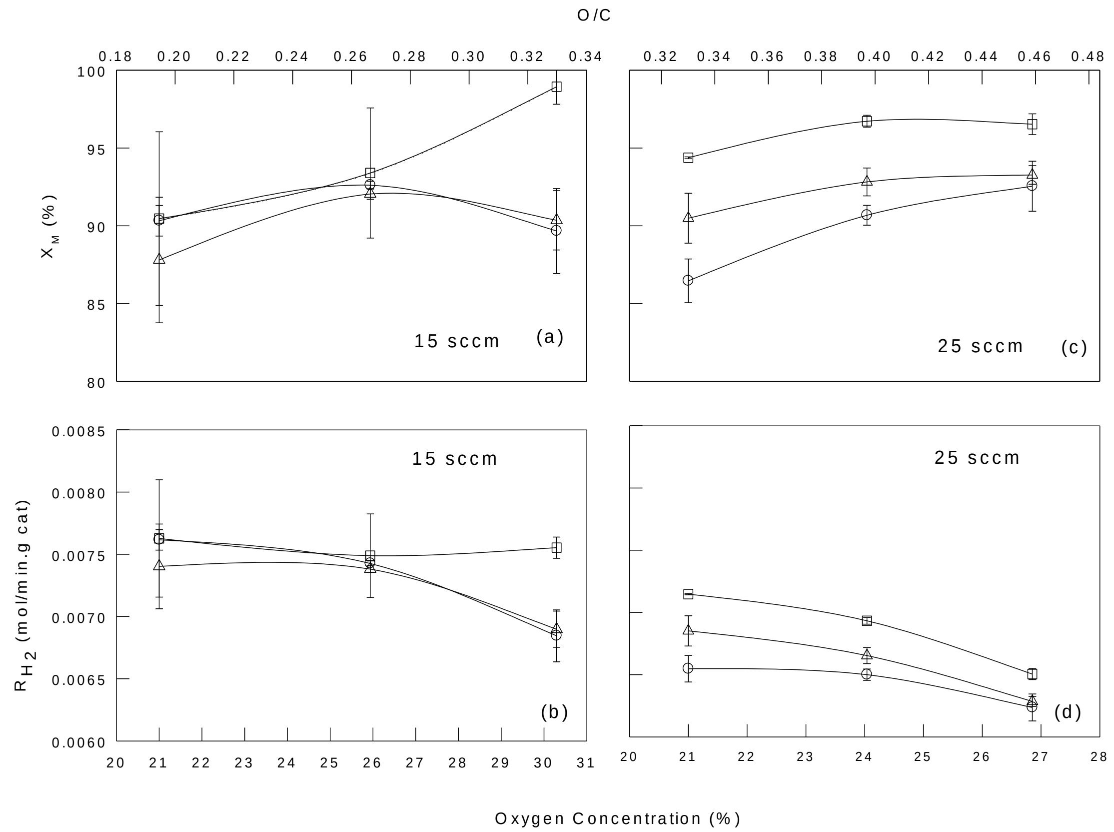

Figure 2. Effect of oxygen concentrations (or ratio of O/C) on catalyst activity measured at various airflow rates and at distinct initial temperatures. T1 = T2 = T4 = 180 °C (○), 190 °C (Δ), and 200 °C (□)

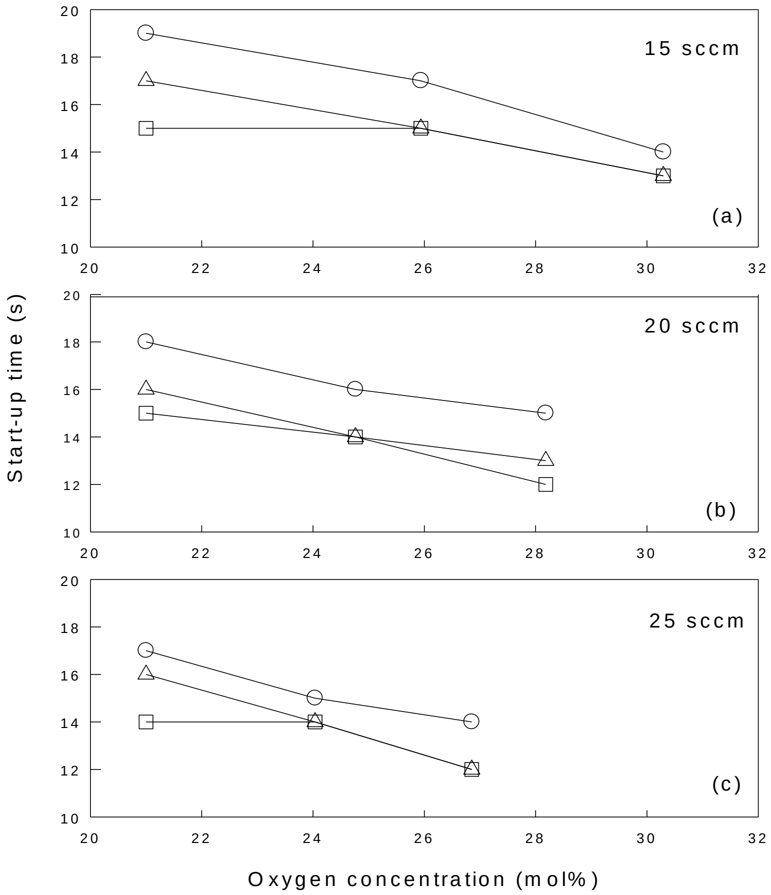

Figure 3. Effect of increasing the oxygen concentration on the startup time when the T3 at $x/L = 0.5$ was 180 °C (○), 190 °C (Δ), or 200 °C (□)

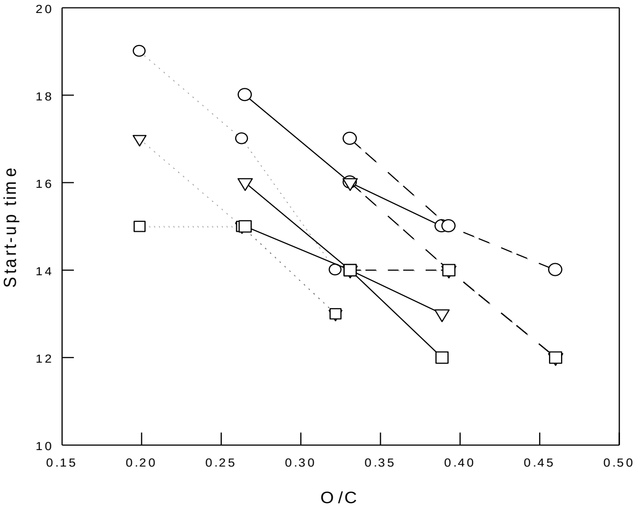

Figure 4. Effect of O/C ratio on the startup time when the T3 at $x/L = 0.5$ was 180 °C (○), 190 °C (▽), and 200 °C (□), and 15 sccm (dotted line), 20 sccm (solid line), 25 sccm (long dash line)

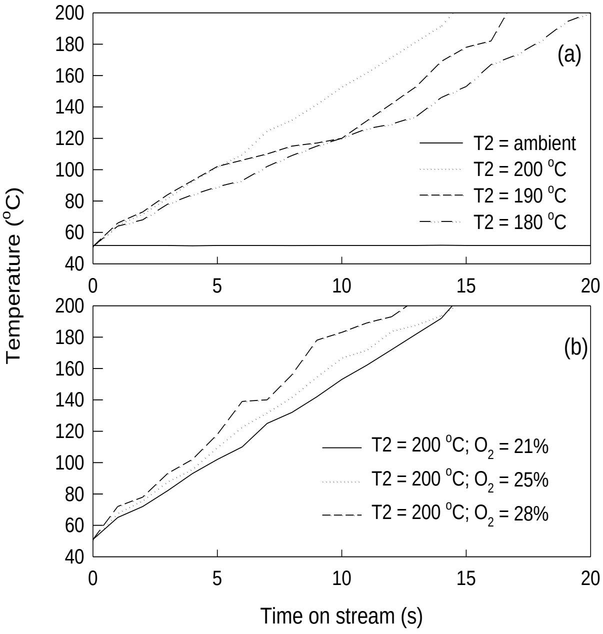

Figure 5. Profile of the temperature (T3) in the catalytic bed according to the time on steam for (a) distinct inlet temperatures (T2) and $[O_2]$ = 21 vol%; and (b) distinct oxygen concentrations and T2 = 200 °C.

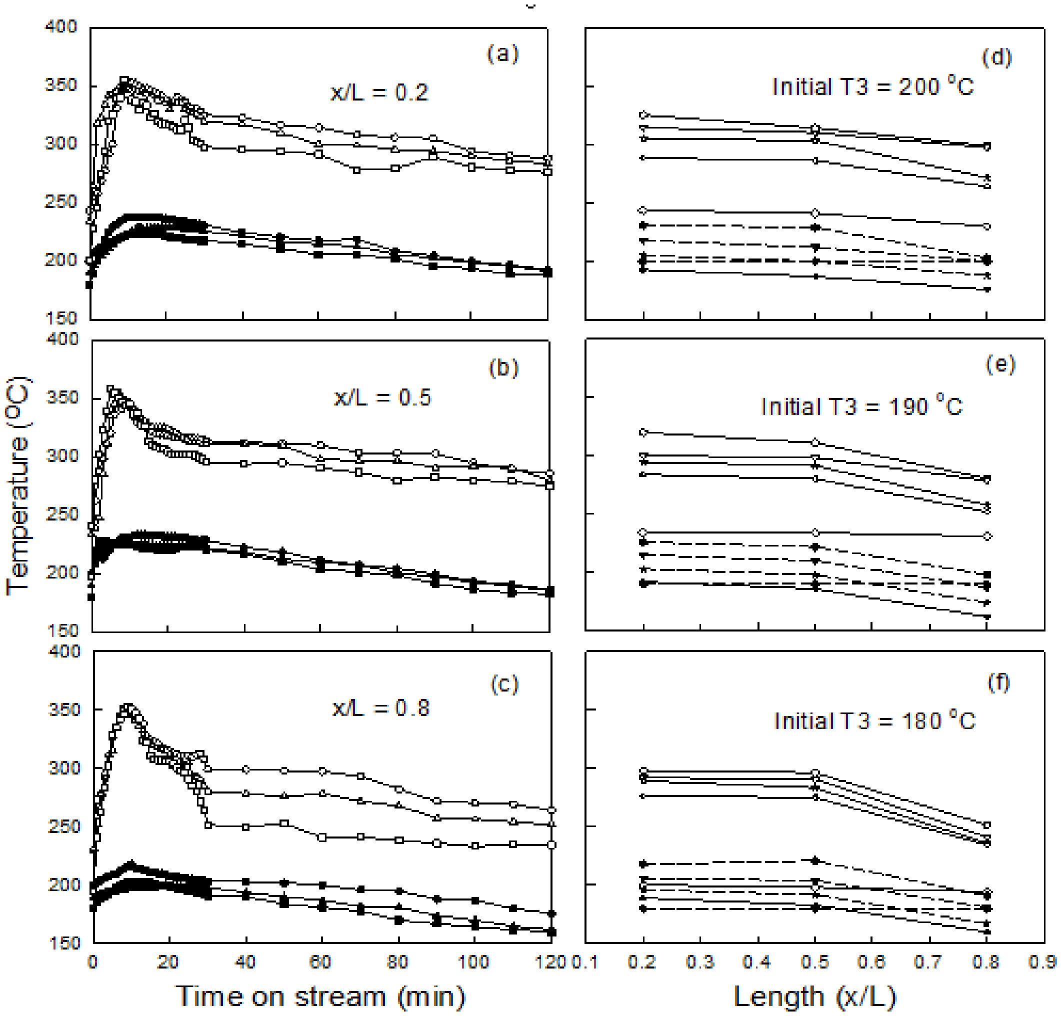

Figure 6. Temperature profiles of T3 and T4 at distinct *x/L* positions in the catalytic bed; (a, b, c) the profiles of T3 and T4 on time on stream for various distinct position T1 = T2 = T3 = 200 °C (○,●), 190 °C (Δ,▲), and 180 °C (□,■); (d, e, f) the profiles of T3 and T4 on the distinct position in the catalytic bed for different initial T3 at reaction time of 0 min (─◇─ , - -◆- -), 30 min (─○─ , – –●– –), 60 min (─▽─ , - -▼- -), 90 min (─☆─ , – –★– –), and 120 min (─✿─ , ─✚─). Catalyst weight = 0.2 g, W/M = 1.2, O/C = 0.27, and WHSV = 6.23 h^{-1}.

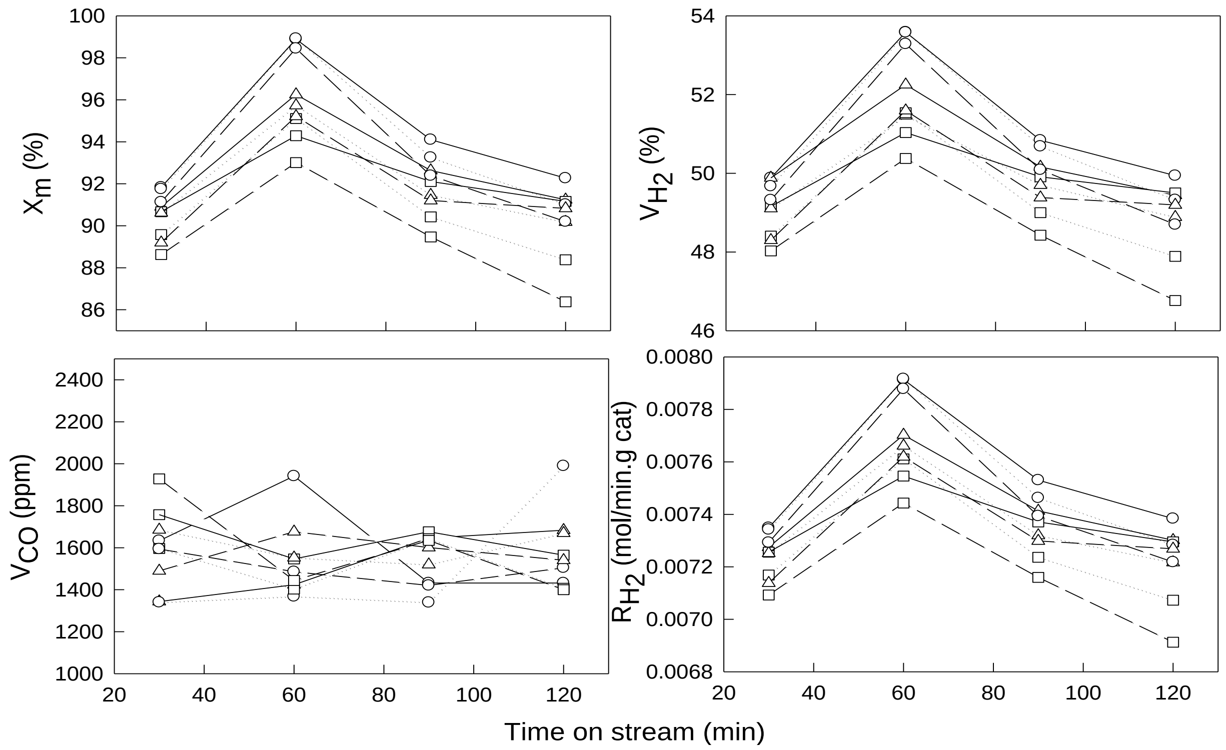

Figure 7. Effect of the initial temperatures of the heating up of the reactants and the catalyst on the catalytic activity measured for the reformation of methanol. Catalyst weight = 0.2 g, W/M = 1.2, O/C = 0.27, and WHSV = 6.23 h^{-1}. T1 = T2 = initial T3 = 200 °C (—○—), 190 °C (—△—), and 180 °C (—□—), at x/L = 0.2; 200 °C (······○······), 190 °C (······△······), and 180 °C (······□······), at x/L = 0.5; and 200 °C (— ○ —), 190 °C (— △ —), and 180 °C (— □ —), at x/L = 0.8.

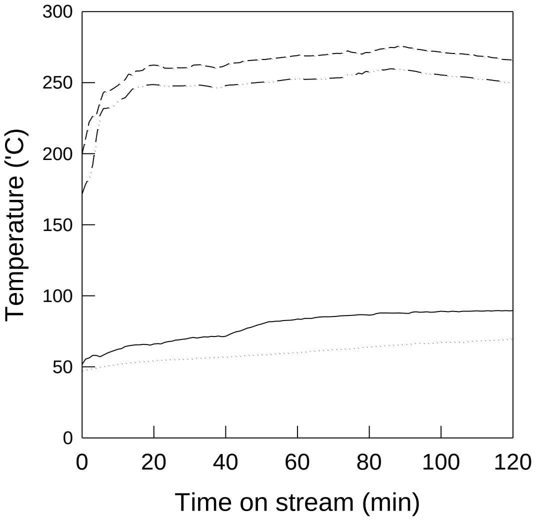

Figure 8. Temperature profiles measured for the catalyst heating up and not heating up under the initial condition in the methanol-reforming reaction; x/L = 0.5, T1 = T2 = 200 °C; (▬ ▬▬ ▬) T3 = (▬•▬) T4 = 25 °C; (▬▬) T3 = (•••••) T4 = 200 °C

Figures 6d-6f present the relationship between initial temperatures of T3 and the temperatures of T3 and T4 during the reaction at various points (x/L) in the catalytic bed; the results show that the greater the length of the catalytic bed (x/L), the lower the temperature. This result indicates that the temperature is not uniform at all points in the catalytic bed and it agrees with the results of Lattner *et al.* [20], who reported that the length of a fixed-bed reactor can be divided into two zones, the oxidation zone and the endothermic reforming-reaction zone. In the oxidation zone, the reaction temperature increases drastically at low reactor length, after which the temperature decreases slowly (and monotonically) with an increase in reactor length, in the so-called endothermic reforming-reaction zone [20].

Figure 7 shows the effect of inlet T2 temperature on methanol conversion and the production of hydrogen and carbon monoxide. The catalytic activity peaked at 60 min into the first reaction, which was observed in the form of high methanol conversion at 60 min; this trend was also observed under the other conditions tested. Maximal methanol conversion was 98%, whereas the maximal hydrogen concentration was 54% and the maximal rate of hydrogen conversion was 7.9×10^{-3} mol/min.g. The minimal concentration of CO was >1300 ppm. Moreover, the high temperature polymer electrolyte membrane FC (PEMFC) with phosphoric acid doped polybenzimidazole was reported high conductivity, good thermal stability and good FC performance at temperature up to 200 ^{o}C. The affinity for CO onto the platinum catalyst is reduced and CO tolerance is increased (e.g., above 160 ^{o}C up to 3% CO can be tolerated in the fuel stream) [21]. The results in this study offers a significant advantage to fuel processing for the high temperature PEMFC and gas cleaning can be removed thus allowing for cost-effective fuel.

3.3. Temperature Profiles of the Catalyst Heating Up and not Heating Up

The ignition temperature on the ATR catalyst depends on several conditions such as the catalyst formulation, structure, composition, and phase, the temperature of the fuel, and the air/fuel ratio (O/C) [12]. Figure 8 shows the temperature profiles (T3 and T4) of the ATR reaction measured for initial T3 values of 50 and 200 °C; T3 and T4 were monitored for 120 min. The maximal T3 measured for initial temperatures of 50 and 200 °C were 90 and 260 °C, respectively, during the 120 min reaction. This result shows that the effect of the ATR reaction (i.e. the ability to generate heat) is correlated with an increase in the temperature in the catalytic bed. Because the reaction temperature increased slowly, a considerable amount of time was required for the (initially low) operational temperature to reach the desired temperature.

Heating the reactants at high temperatures increased the temperature in the catalytic bed. T3 rose sharply when the reaction time was < 20 min, and then remained stable for up to 300 min of the reaction. When the initial T3 was 50 °C, the methanol conversion remained at around 9% during the 300-min reaction.

4. Conclusions

Oxygen enrichment is a promising method that can be used for increasing methanol conversion in the ATR process. However, the results of this study indicate that increasing the oxygen concentration lowers the hydrogen concentration; consequently, the concentration of carbon monoxide is high (1300 ppm). A high oxygen concentration can reduce the startup time when $Cu/ZnO/Al_2O_3/Cr_2O_3/Ce_2O_3$ (42.9:42.9:7.14:3.57:3.57 wt.%) is used as the catalyst, and the minimal startup attained is 12 s. An increase in the concentration of oxygen correlates with an increase in the temperature of the catalytic bed. The temperature of a fixed-bed catalyst is a function of x/L (the length of the fixed-bed catalyst). The temperature profile measured for the fixed-bed reactor is not the same at various lengths of the reactor (x/L). The temperature of the bed catalyst is decreased substantially when x/L is large .

Acknowledgement

The authors thank the National Science Council of Taiwan for financially supporting this research under grant numbers NSC 100-2221-E-155-037-MY2, and also thank Professors Chi-Yuan Lee, Chia-Chieh Shen, Kuen-Song Lin, and Yu-Chuan Lin of Yuan Ze University for their valuable advice on and assistance in the experiments.

References

[1] Lesmana, D., Wu, H.S. (2012). Short Review: Cu Catalyst for Autothermal Reforming Methanol for Hydrogen Production. *Bulletin Chemical Reaction Engineering & Catalysis*. 7: 27-42. (DOI: 10.9767/bcrec.7.1.1284.27-42)

[2] Lin, K.S., Pan, C.Y., Chowdhury, S., Tu, M.T., Hong, W.T., Yeh, C.T. (2011). Hydrogen Generation Using a $CuO/ZnO-ZrO_2$ Nanocatalyst

for Autothermal Reforming of Methanol in a Microchannel Reactor. *Molecules*. 16: 348-366.

[3] Chin, Y.H., Dagle, R., Hu, J., Dohnalkova, A.C., Wang, Y. (2002) Steam Reforming of Methanol over Highly Active Pd/ZnO Catalyst. *Catalysis Today*. 77: 79-88.

[4] Agrell, J., Birgersson, H., Boutonnet, M., Cabrera, I.M., Navaro, R.M., Fierro, J.L.G. (2003). Production of Hydrogen from Methanol over Cu/ZnO Catalyst Promoted by ZrO_2 and Al_2O_3. *Journal of Catalysis*. 219: 389-403.

[5] Prins, M.J., Ptasinski, K.J., Janssen, J.J.G. (2007). From Coal to Biomass Gasification: Comparison of Thermodynamic Efficiency. *Energy*. 32: 1248-1259.

[6] Turco, M., Bagnasco, G., Cammarano, C., Senese, P., Costantino, U., Sisani, M. (2007). $Cu/ZnO/Al_2O_3$ Catalysts for Oxidative Steam Reforming of Methanol: The Role of Cu and The Dispersing Oxide Matrix. *Applied Catalysis B: Environmental*. 77: 46-57.

[7] Kuo, C.H., Lesmana, D., Wu, H.S. (2013) Hydrogen Production of Methanol Reformation Using $Cu/ZnO/Al_2O_3$ Catalyst at Low Temperature. *Bulletin Chemical Reaction Engineering & Catalysis*. 82: 110-124. (DOI: 10.9767/bcrec.8.2.4844.110-124)

[8] Chang, C.C., Chang, C.T., Chiang, S.J., Liaw, B.J., Chen, Y.Z. (2010). Oxidative Steam Reforming of Methanol Over $CuO/ZnO/CeO_2/ZrO_2/Al_2O_3$ Catalysts. *International Journal of Hydrogen Energy*. 35: 7675-7683.

[9] Patel, S., Pant, K.K. (2007). Hydrogen Production by Oxidative Steam Reforming of Methanol Using Ceria Promoted Copper-alumina Catalysts. *Fuel Processing Technology*. 88: 825-832.

[10] Nahar, G., Dupont, V. (2013). Recent Advances in Hydrogen Production via Autothermal Reforming Process (ATR): A Review of Patents and Research. *Recent Patents on Chemical Engineering*. 6: 8-42.

[11] Hernandez, R.P., Martinez, A.G., Wing, C.E.G. (2007). Effect of Cu Loading on CeO_2 for Hydrogen Production by Oxidative Steam Reforming of Methanol. *International Journal of Hydrogen Energy*. 32: 2888-2894.

[12] Ahmed, S., Ahluwalia, R., Lee, S.H.D. (2003). Experimental Study to Determine Fast-start Capability of On-board Fuel Processors. *Fuel Cell Seminar Abstracts*. Miami Beach, FL, 2003.

[13] Springmann, S., Bohner, M., Sommer, M., Himmen, M., Eigenberger, G. (2003). Steady State and Dynamic Simulation of an Autothermal Gasoline Reformer. *Chemical Engineering Technology*. 26: 790-796.

[14] Coombe, H.S., Nieh, S. (2007). Polymer Membrane Air Separation Performance for Portable Oxygen-enriched Combustion Application. *Energy Conversion and Management*. 48: 1499-1505.

[15] Baker, R.W. (2002). Future Directions of Membrane Gas Separation Technology. *Industrial Engineering Chemical Research*. 4: 1393-1411.

[16] Bingue, J.P., Saveliev, A.V., Kennedy, L.A. (2004). Optimization of Hydrogen Production by Filtration Combustion of Methane by Oxygen Enrichment and Depletion. *International Journal of Hydrogen Energy*. 29: 1365-1370.

[17] Newson, E., Truong, T.B. (2003). Low-temperature Catalytic Partial Oxidation of Hydrocarbons (C_1-C_{10}) for Hydrogen Production. *International Journal of Hydrogen Energy*. 28: 1379-1386.

[18] Lesmana, D., Wu, H.S. (2014). Modified Oxalic Acid Co-precipitation Method for Preparing $Cu/ZnO/Al_2O_3/Cr_2O_3/CeO_2$ Catalysts for the OR (oxidative reforming) of M (methanol) to Produce H_2 (Hydrogen) Gas. *Energy*. 69: 769-777.

[19] Wu, H.S., Chung, S.C. (2007). Kinetics of Hydrogen Production of Methanol Reformation Using $Cu/ZnO/Al_2O_3$ Catalyst. *Journal of Combinatorial Chemistry*. 9: 990-997.

[20] Lattner, J.R., Harold, M.P. (2007) Autothermal Reforming of Methanol: Experiments and Modeling. *Catalysis Today*. 120:78-89.

[21] Chandan, A., Hattenberger, M., El-kharouf, A., Du, S., Dhir, A., Self, V., Pollet, B. G., Ingram, A., Bujalski, W. (2013). High Temperature (HT) Polymer Electrolyte Membrane Fuel Cells (PEMFC) - A Review. *Journal of Power Sources*. 231: 264-278.